Journal of Pharmaceutical and Biomedical Analysis 55 (2011) 23–30

Contents lists available at ScienceDirect

Journal of Pharmaceutical and Biomedical Analysis

journal homepage: www.elsevier.com/locate/jpba

Qualitative on-line profiling of ceramides and cerebrosides by high performance liquid chromatography coupled with electrospray ionization ion trap tandem mass spectrometry: The case of *Dracontium loretense*

Assunta Napolitano, Angelyne Benavides, Cosimo Pizza, Sonia Piacente*

Dipartimento di Scienze Farmaceutiche, Università degli Studi di Salerno, Via Ponte Don Melillo, I-84084 Fisciano, SA, Italy

ARTICLE INFO

Article history:
Received 28 September 2010
Received in revised form
21 December 2010
Accepted 23 December 2010
Available online 13 January 2011

Keywords:
Ceramide
Cerebroside
HPLC–ESI/ITMS profiling

ABSTRACT

Ceramides and cerebrosides are key compounds in the metabolism of sphingolipids. Produced in response to a variety of apoptotic stimuli, these metabolites mediate either mitogenic or apoptotic responses, depending on cell type and nature of stimulus. Novel strategies using these selective targets for a therapeutic intervention, e.g. in cancer, cardiovascular and neurodegenerative diseases, and HIV, have been developed, along with anticancer approaches using controlled delivery of exogenous natural ceramides from ceramide-based liposomes. Thus, great is the need to find selective and sensitive analytical methods allowing a prompt detection of ceramides and cerebrosides in natural matrices. Here we report an analytical study carried out on the Amazonian plant *Dracontium loretense*, resulted in a preliminary analysis a rich source of this class of natural compounds. A handy, selective, and sensitive methodology based on high-performance liquid chromatography coupled to electrospray negative ionization multistage ion trap mass spectrometry (HPLC–ESI/ITMS^n) was developed. Analysis of fingerprint multistage mass spectra allowed the rapid identification of 3 major long-chain bases and their exact pairing with 11 different fatty acids and with carbohydrate headgroups. Thus, the structures of 21 ceramide and cerebroside species, among which 7 molecules never reported before, were unambiguously assigned. Results obtained in this study demonstrated that this analytical approach could provide a reliable and sensitive method to obtain the qualitative on-line profiling of ceramides and cerebrosides in new medicinal plant matrices.

1. Introduction

Ceramides and cerebrosides (glycosphingolipids consisting of a ceramide with a single sugar residue, usually glucose or galactose, at C-1) are lipid molecules with a sphingoid base backbone, and represent key compounds in the metabolism of sphingolipids [1]. Produced in response to a variety of apoptotic stimuli, these metabolites mediate either mitogenic or apoptotic responses, depending on cell type and the nature of the stimulus [2]. In particular, ceramides are receiving much attention as important second messengers for various cellular processes, including apoptosis, proliferation, migration and senescence [3]. Moreover, cerebrosides, metabolic intermediates in the anabolic and catabolic pathways of complex glycosphingolipids, are standing out for their cytotoxic, anti-HIV-1, neuritogenic, hepatoprotective, and immunostimulatory activities [4–6]. Furthermore, β-glucosylceramide isolated from malt feed has shown to inhibit the growth of cancer cells, to decrease the tumor metastasis of lymphoma cells, and to induce antitumor immunity *via* activation of natural killer T (NKT) cells *in vivo* [3,7]. Accordingly, results of recent studies have suggested that β-structured glycosphingolipids are potent NKT cell ligands [4]. Besides, β-glycosphingolipids have been reported to show beneficial effects in NKT cell-dependent immune-mediated metabolic and malignant animal models *in vivo* [3,4]. Thereby, novel strategies using these selective targets for a therapeutic intervention, e.g. in cancer, cardiovascular and neurodegenerative diseases, and HIV, have been adopted. Furthermore, anticancer approaches using exogenous application of short-chain ceramides, or controlled delivery of exogenous natural ceramides from ceramide-based liposomes, have been explored, showing an antitumor activity *in vivo* [2,8–10]. Analogously, delivery of ceramide and glucosylceramide sphingolipids from dietary sources has been applied as strategy to accumulate naturally-occurring long acyl chain ceramides in tumor cells, suggesting these compounds like functional food components having chemopreventive effects [7,8,11]. Thereby the interest in developing prompt, selective and sensitive analytical methods to detect bioactive ceramides and cerebrosides in natural matrices as new sources of supply is increasing.

In our continuing research for bioactive secondary metabolites, we have previously carried out the phytochemical study of

* Corresponding author. Tel.: +39 089969763; fax: +39 089969602.
E-mail address: piacente@unisa.it (S. Piacente).

0731-7085/$ – see front matter © 2011 Elsevier B.V. All rights reserved.
doi:10.1016/j.jpba.2010.12.035

Dracontium loretense Engl. (Araceae), for which there was no phytochemical investigation, despite its biological activities and its large worldwide marketing [12]. In particular, the infusion obtained from *D. loretense* (trivial name "jergón sacha") together with extract or infusion from *Uncaria tomentosa* is traditionally used by AIDS patients to reinforce immune system [13]. In agreement with the described property to enhance the immune function, a recent pharmacological study on different South American herbal extracts reports the ability of the ethanol extract of *D. loretense* to reduce the aggravation of clinical symptoms in a mouse model of experimental autoimmune encephalomyelitis (EAE) by inhibition of T helper 1 cells [14]. Interestingly a preliminary analysis by ESI-ITMS^n direct injection of the butanol extract of *D. loretense* corms highlighted the presence, as main constituents, of ceramides and cerebrosides. Since there is a limited number of studies concerning the structural analysis of glucocerebrosides and ceramides from medicinal and food plants, we decided to perform an investigation on this natural matrix with the aim to obtain a qualitative profiling of these metabolites, developing a general, selective and sensitive analytical method to structurally analyze ceramide and cerebroside compounds in complex plant mixtures.

The isolation and identification of plant ceramides and cerebrosides by conventional procedure are generally tedious and time-consuming, frequently due to their low contents in these matrices [1,15–17]. Besides, the structural variability of sphingolipid classes poses special problems for their analysis, above all the impossibility to use ultraviolet detection for analytical purpose, due to the lack of a chromophore [17]. In most cases, sphingolipid molecules have been mainly analyzed by TLC, HPLC, GC, MS or GC–MS following acid or alkaline hydrolysis of the extracts and derivatization, losing structural information by hydrolysis of the linkage positions [17–19]. Considering that the biological activity varies with the structure, information about intact molecular species is very important.

A powerful tool for structural elucidation and analysis of complex intact sphingolipids is the on-line combination of high-performance liquid chromatography with mass spectrometry, which provides structure specific data for the characterization of known or unknown molecular species. Liquid chromatography allows complex mixtures of sphingolipids from crude extracts to be trapped, focused, and selectively eluted prior to introduction into the mass spectrometer. Tandem mass spectrometry uniquely identifies various types of sphingolipids by characteristic fragmentations of either head group, or fatty acid, or sphingoid base. Thereby, coupling the sensitivity and specificity of the mass spectrometer to the equally powerful and effective analytical technique of HPLC increases the resolving power of the analysis and provides rapid, robust, sensitive, and highly specific levels of analyte identification. Nevertheless, while the emerging field of sphingolipidomics has received much attention in animal biology, it remains neglected in plants [20]. In fact, in the last years only few reports describing the investigation of sphingolipids in plants by HPLC–MS were published [17,21–23]. With the exception of one report describing an HPLC–ESIMSMS method operating in both ionization ion mode on a QTrap instrument, most of them made use of HPLC–MS methods based on positive ionization ion mode by APCI or particle beam sources on single quadrupole instruments operating in chemical ionization mode using in source collision-induced dissociation (CID), or by TurboIonSpray on QTrap mass spectrometer operating in MSMS scan mode. In any case, these HPLC–MS methods, yielding poor ceramide fragmentation data, did not provide a large and complete sphingolipid structural information to promptly and unambiguously assign the ceramide long chain base and acyl-chain moieties. Thereby, since up to now no systematic study *via* high-performance liquid chromatography coupled to electrospray negative ionization multistage ion trap mass spectrometry (HPLC–ESI/ITMS^n) for a complete characterization of ceramides and cerebrosides from plant matrices has been reported, the present study has been aimed to develop a prompt, selective, and sensitive analytical method based on HPLC–ESI/ITMS^n to obtain the qualitative on-line profiling of *D. loretense* corms relative to this class of compounds. The fragmentation mechanisms of two representative sphingolipids were investigated in detail using ESI negative ionization multistage mass spectrometry equipped with an ion trap instrument. On the basis of the obtained structural information, a rapid, simultaneous and unambiguous structure identification of the individual constituents occurring in the *D. loretense* corms, including 7 compounds never reported before, was obtained by the analysis of the relative fingerprint multistage mass spectra, giving information about the long-chain sphingoid base as well as the fatty acid moiety.

2. Experimental

2.1. Chemicals and reagents

HPLC-grade acetonitrile (ACN) was purchased from Merck (Darmstadt, Germany). Dracontioside A and B (**5**, **14**) were isolated from the corms of *D. loretense*. Their structures were fully identified by NMR and MS spectroscopy. Deionized water purified by a Millipore Milli-Q system (Bedford, MA, USA) was used throughout the experiment. Other solvents were of analytical grade.

2.2. General experimental procedures

^{1}H and ^{13}C NMR spectra were recorded on a Bruker DRX-600 spectrometer equipped with a Bruker 5 mm TCI cryoprobe; chemical shifts were referenced to the residual solvent signal (methanol-d_4, $\delta_H = 3.34$, $\delta_C = 49.0$). The ^{1}H, gCOSY, gHSQC, and gHMBC NMR experiments were run under standard conditions at 300 K. ESIMS and ESIMS^n analyses of standard cerebrosides were performed on an LCQ Deca ion trap mass spectrometer (ThermoFinnigan, San Jose, CA, USA). To optimize the mass spectrometric parameters, each standard dissolved in CH_3OH (10 $\mu g\,ml^{-1}$) was infused in the ESI source by a syringe pump (flow rate 5 μl/min) and analyzed in negative ion mode. The optimized parameters were: capillary voltage −41 V, spray voltage 5 kV, tube lens offset 35 V, capillary temperature 280 °C, and sheath gas (nitrogen) flow rate 40 (arbitrary units). To optimize the ESIMS^n conditions, the collision energy percentage was increased up to 40 to produce a whole fragmentation pattern showing an array of all possible fragments. Butanol extract and enriched ceramide and cerebroside samples were analyzed by on-line HPLC–ESI/ITMS^n using a ThermoFinnigan Spectra System HPLC (ThermoFinnigan, San Jose, CA, USA) coupled with the mass spectrometer. HPLC separation was conducted on a RP C4 column (3.5 μm, 2.1 mm × 150 mm; Symmetry 300 C4; Waters, Milford, MA) at a flow rate of 0.2 ml/min. A gradient elution was performed by using H_2O (A) and CH_3CN (B), both added of 0.1% acetic acid, as mobile phases, and following gradient steps: from 40% B to 50% B in 5 min; to 77% B in 27 min; hold to 77% B for 13 min; 70 100% B in 5 min. The column effluent was analyzed by ESIMS and ESIMS^n in negative ion mode according to the optimized parameters indicated for the direct injection with the auxiliary gas (nitrogen) supplied at a flow rate of 10 (arbitrary units). Data were acquired in MS^1 and MS^n scanning modes and processed using the software provided by the manufacturer. Column chromatography was performed over Sephadex LH-20 (Pharmacia). HPLC separations were carried out on a Waters System, equipped with a refractive index detector, a μ-bondapack C_{18} column (300 mm × 7.6 mm i.d., 10 μm), and a Rheodyne injector. TLC was performed on silica gel F254 (Merck) plates.

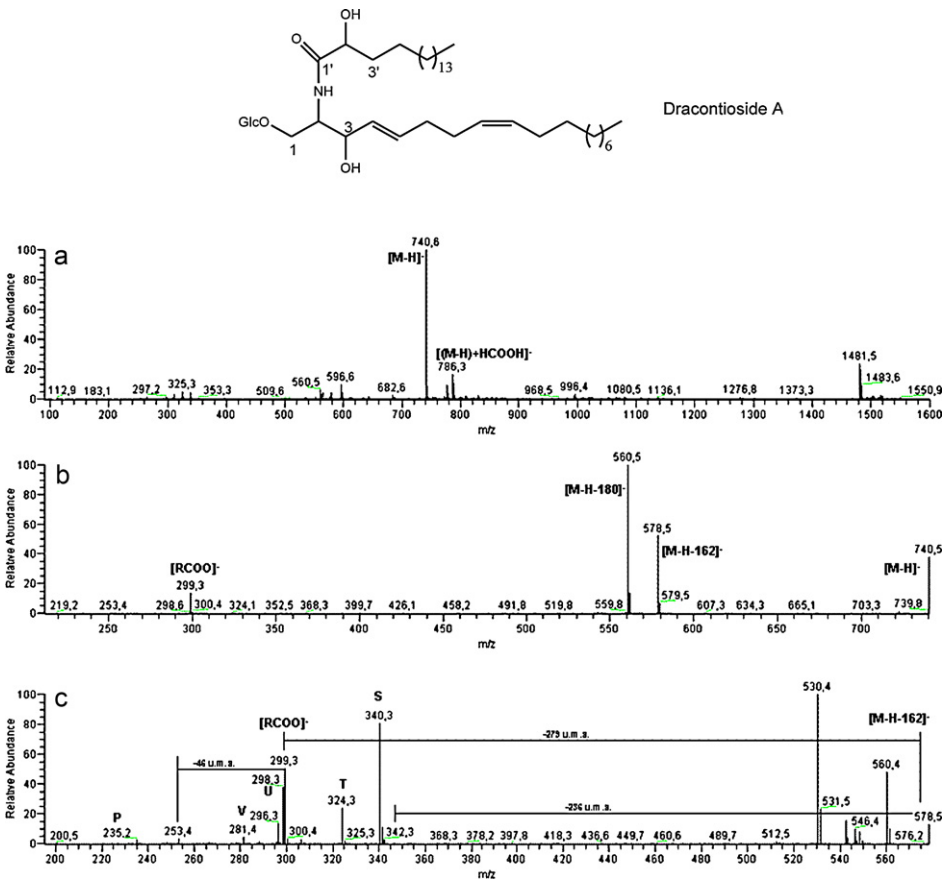

Fig. 1. (a) Full negative ESIMS spectrum of dracontioside A; (b) negative ESIMS^2 spectrum of [M−H]$^-$ precursor ion; (c) negative ESIMS^3 spectrum of [M−H−162]$^-$ product ion.

2.3. Plant material

D. loretense corms were collected in Iquitos, Peru, in May 2005. The plant material was identified by the biologist Elsa Rengifo (Instituto de Investigaciones de la Amazonía Peruana – IIAP). A voucher specimen has been deposited in the Herbarium of the Department of Pharmacognosy, Faculty of Pharmacy, Universidad Nacional Mayor de San Marcos, Lima, Peru.

2.4. Sample preparation procedures

Dried and powdered corms (800 g) of *D. loretense* were extracted for a week, three times, at room temperature using solvents of increasing polarity, namely, petroleum ether 1.5 l, chloroform 1.5 l, and methanol 1.5 l. The extractive solutions were evaporated to dryness in vacuo to give 0.4 g, 1.3 g, and 57.6 g of crude extract, respectively. The methanol extract was partitioned between water and butanol (1:1), yielding 6.3 g of butanol extract. 3 g of this extract were fractionated on a Sephadex LH-20 column (100 cm × 5 cm) using methanol as mobile phase, obtaining an enriched ceramide and cerebroside sample (fractions 12–15, 0.8 g), as confirmed by ESIMS^n analyses. The purification of this sample by isocratic HPLC using CH_3OH/H_2O (93:7, v/v) as eluents (flow rate of 2 ml/min) yielded dracontioside A (4.3 mg, t_R = 15 min) and dracontioside B (1.6 mg, t_R = 38 min).

3. Results and discussion

3.1. Fragmentation behaviour of dracontioside A and B used as standard compounds

Structure variability of plant sphingolipids principally consists in the different nature of sphingolipid base, fatty acid unit, and sugar moiety which make up these metabolites. Sphinganine, 4-hydroxysphinganine, *cis* and *trans* isomers of 8-sphingenine, 4,8-sphingadienine, and 4-hydroxy-8-sphingenine, all sharing a 2-amino-1,3-dihydroxy octadecane core structure, are the most representative plant long-chain bases [24]. Plant fatty acids are predominantly α-hydroxylated and usually have a length from 16 to 26 carbon atoms. They are amide-linked to the sphingoid base of complex plant ceramides and glucocerebrosides, and may be saturated or unsaturated long-chain odd- and even-numbered. Finally, cerebroside compounds exhibit an hexose, or another carbohydrate, as polar headgroup bound to a ceramide by a glycosidic linkage in position 1.

Therefore, in order to structurally define ceramides and cerebrosides occurring in *D. loretense* corms, a fractionation procedure of the butanol extract was applied yielding a sample enriched in target molecules, from which two standard substances, named dracontioside A and B, were obtained. The fragmentation patterns of the two standards, each belonging to classes of sphingolipids differing for sphingolipid base and fatty acid nature (Figs. 1 and 2), were studied.

To obtain best sensitivity optimizing the mass spectrometric parameters, each compound was infused into the ESI source and analyzed on an ion trap instrument in negative ionization mode. In this conditions, cerebroside compounds mainly yielded [M−H]$^-$ ions, together with three further signals of lower intensity, [(M−H)+CH_3COOH]$^-$, [(M−H)+HCOOH]$^-$, and [(M−H)+CF_3COOH]$^-$ ions, due to the formation of adducts with acetic, formic and trifluoroacetic acids, respectively, with the latest two being contaminations from previous experiments. These acid adducts, disappearing in different tune conditions, were useful diagnostic ions as sphingolipid selective markers.

Negative ESIMS^n product ion spectra recorded for each standard provided an optimum of structural information about the fatty acid

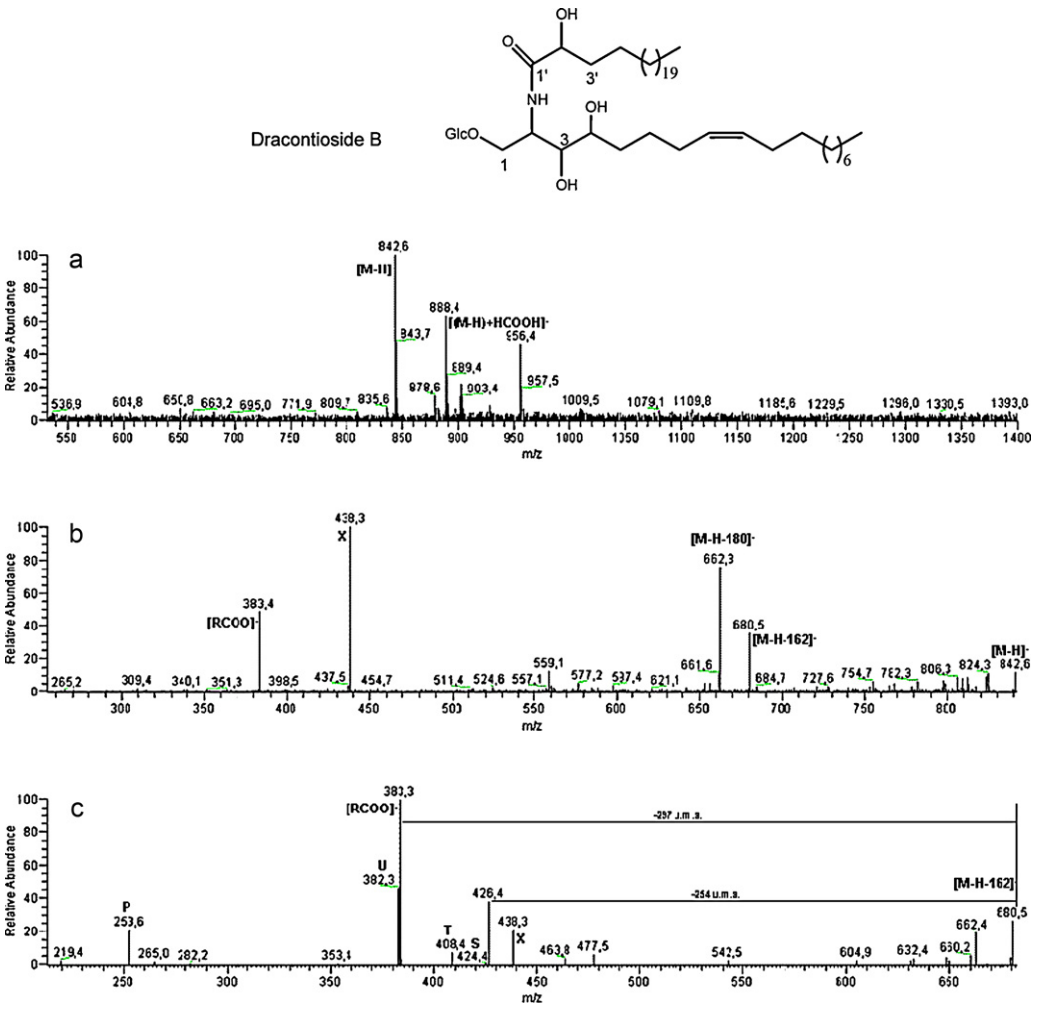

Fig. 2. (a) Full negative ESIMS spectrum of dracontioside B; (b) negative ESIMS^2 spectrum of $[M-H]^-$ precursor ion; (c) negative ESIMS^3 spectrum of $[M-H-162]^-$ product ion.

as well as the long-chain base moiety, mainly yielding two groups of product ions, those relative to the long-chain base, and those referring to the acyl component. In this regard, the analysis of the ESIMS^3 spectra acquired on dracontioside A and B $[(M-162)-H]^-$ product ions showed the presence of peak ions originating by the neutral loss of 279 or 297 amu, respectively, allowing to immediately discriminate about the presence of a cerebroside molecule containing a 4,8-sphingadienine or a 4-hydroxy-8-sphingenine as long-chain base, and to identify the product ion relative to the fatty acid moiety (Fig. 3).

Analogous conclusions could be achieved checking, in the same spectra, product ions originated from $[(M-162)-H]^-$ ions by the cleavage between C2 and C3 or C3 and C4 carbon atoms on the *N*-acylated-sphingoid base, and producing neutral losses of 2,6-hexadecadienal (M.W. 236 amu), or 2-hydroxy-6-hexadecenal and 5-pentadecenal aldehyde (M.W. 254 and 224 amu), respectively (Fig. 3). In addition to peak ions originated by described neutral losses, ESIMS^3 spectra showed characteristic fragment ions giving further information about the identity of the sphingoid chain. Thereby, in agreement with the literature reports and with previous nomenclature proposed for detected fragment ions [25–28], peak ions corresponding to the P and Q product ions were detected (Fig. 4). Moreover, as already specified, negative ESIMS^3 spectra yielded also a set of product ions referring to the acyl component. Fragment ions relative to fatty acid and V anions were particularly evident, giving rapid information about the molecular weights of the fatty acyl groups. Finally, complementary information on both sphingoid chains and fatty acids was obtained by observing the presence of U, T, S, X, and W product ions, corresponding to fragment ions containing fatty acyl chain bounded to part of sphingoid base (Figs. 1 and 2).

In detail, the full negative ESIMS spectrum of dracontioside A showed a main $[M-H]^-$ ion peak at *m*/*z* 740, together with the minor $[(M-H)+HCOOH]^-$ adduct ion at *m*/*z* 786 (Fig. 1). The collision induced dissociation (CID) of the negative $[M-H]^-$ precursor ion at *m*/*z* 740 yielded the $[M-H-162]^-$ and $[M-H-180]^-$ product ions at *m*/*z* 578 and *m*/*z* 560, due to the neutral loss of an hexose unit from the precursor ion and confirming the glycosylated nature of dracontioside A (Fig. 4). Particularly informative was the ESI-MS^3 spectrum of the product ion at *m*/*z* 578, showing the characteristic neutral loss of 279 amu, along with P, S, T, U, and W fragment ions, which allowed the determination of the long-chain base as a 4,8-sphingadienine (Fig. 1). The presence in ESI-MS^2 and ESIMS^3 spectra of the fragment ion at *m*/*z* 299, originated from the $[M-H-162]^-$ ion by neutral loss of the 1-dehydroxy-1,4,8-sphingetrienine (M.W. 279 amu), and due to the acyl-chain anion, allowed to define the nature of the fatty acid as a 2-hydroxy-octadecanoic acid. On the other hand, the ESIMS^3 analysis of the fragment ion at *m*/*z* 299 highlighted the presence of the product ion at *m*/*z* 253, originating by a neutral loss of 46 Da and diagnostic for the typical dissociation pathway of an α-hydroxy fatty acid in tandem mass spectrometric experiments

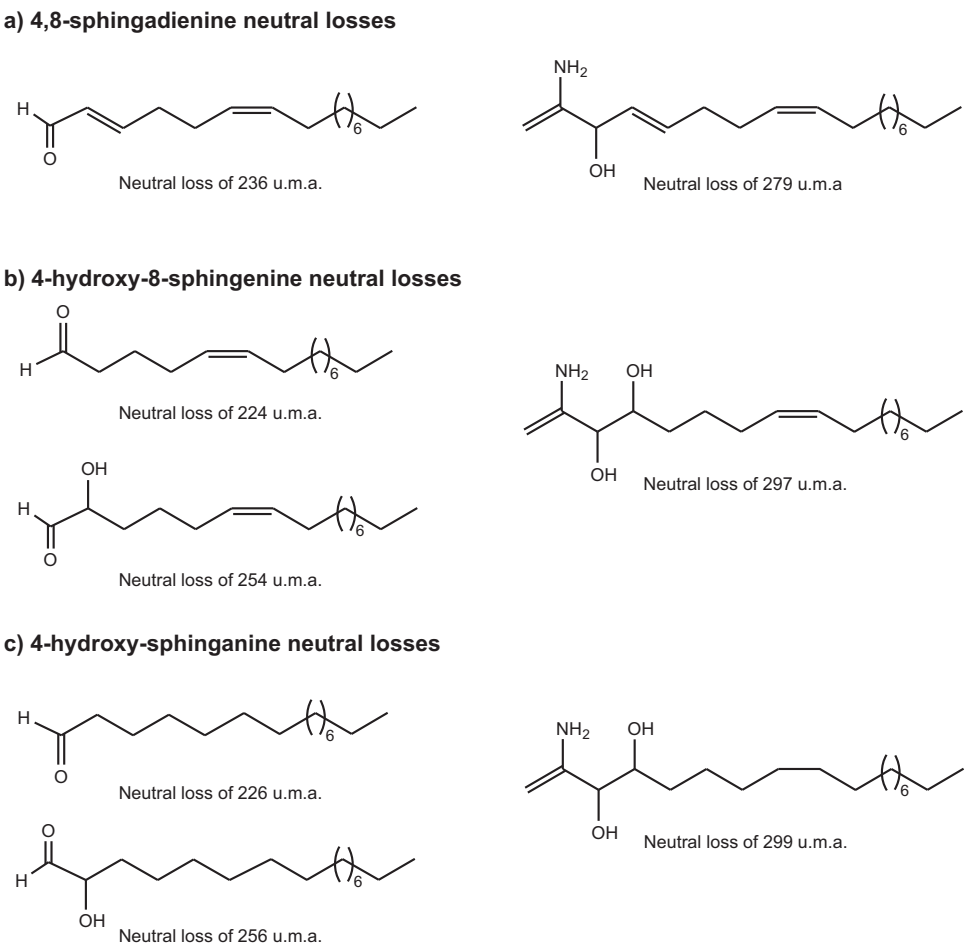

Fig. 3. Sphingoid base neutral losses occurring in ESIMS^n experiments.

[29]. Therefore, the analysis of acquired mass spectrometric data permitted to identify dracontioside A as 1-*O*-glucopyranosyl-2-*N*-2′-hydroxyhexadecanoyl-4,8-sphingadienine, a compound already isolated from *Arisaema amurense*, a perennial herb belonging to Araceae family [6,30].

The negative ESIMS^n product ion spectra of dracontioside B showed a similar fragmentation pattern as obtained for dracontioside A, differing only for the presence, in ESI-MS^3 spectrum of the $[(M-162)-H]^-$ product ion at *m*/*z* 680, of a diagnostic product ion at *m*/*z* 383, due to the fatty acid anion,

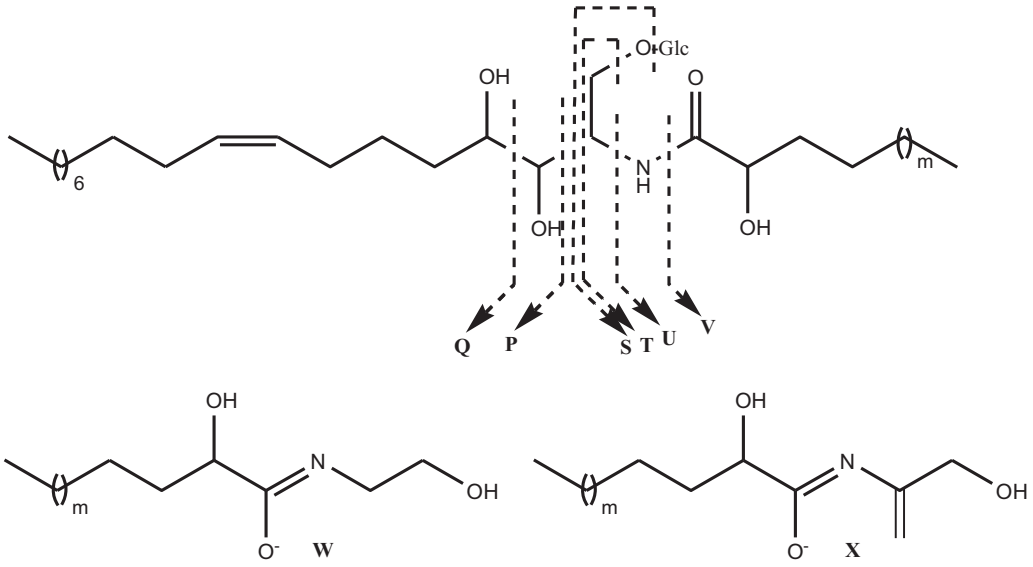

Fig. 4. Characteristic fragment ions originated from a cerebroside having a 4-hydroxy-8-sphingenine long-chain base.

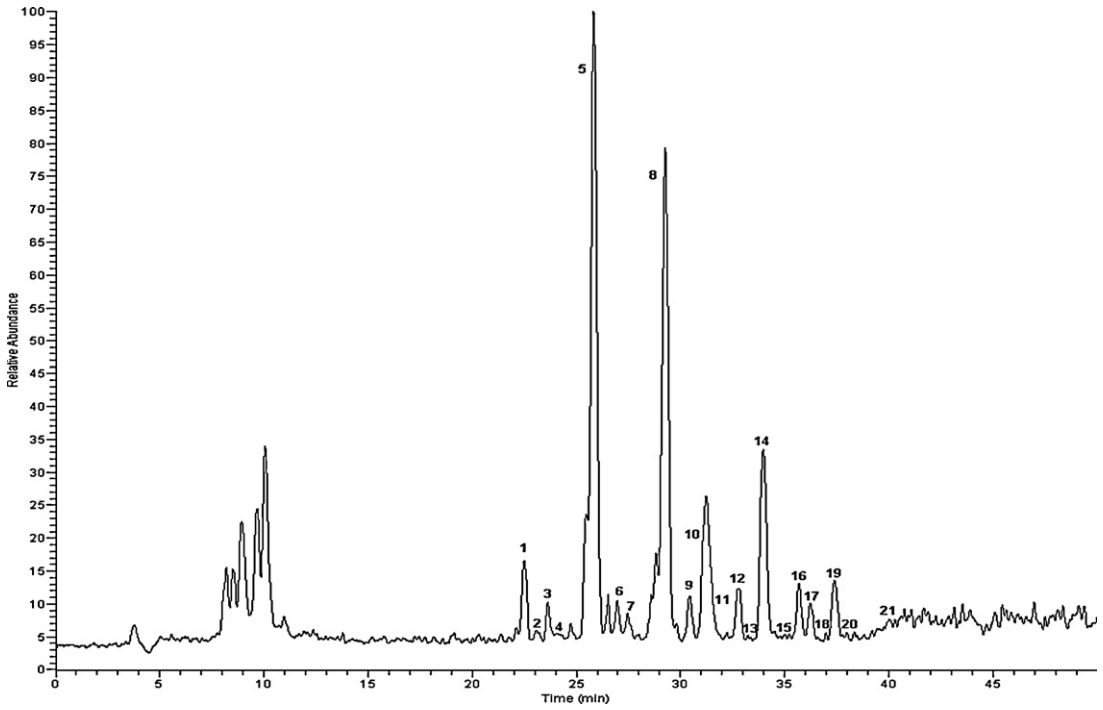

Fig. 5. HPLC–ESI/ITMS profile of ceramides and cerebrosides of *D. loretense* corms.

and generated by the neutral loss of 297 amu, corresponding to 1-dehydroxy-4-hydroxy-1,8-sphingedienine (Fig. 2). The presence of this product ion was at the same time indicative both of a 4-hydroxy-8-sphingenine long-chain base and of a 2-hydroxy-tetracosanoic acid. Thereby, dracontioside B could be assigned as a 1-*O*-glucopyranosyl-2-*N*-2′-hydroxytetracosanoyl-4-hydroxy-8-sphingenine, previously isolated from *Euphorbia sororia* [31].

3.2. Identification of ceramide and cerebroside compounds from *D. loretense*

In order to study the general chromatographic behaviour and to provide a simultaneous and unambiguous on-line structure identification of ceramide and cerebroside compounds occurring in *D. loretense* corms, the butanol extract was analyzed by HPLC–ESI/ITMS^n, using the same conditions described for ESIMS^n analyses, aqueous acetonitrile with addition of 0.1% of acetic acid as mobile phase, and reversed phase (RP) instead of normal phase HPLC because of the better compatibility with ESIMS. To optimize HPLC conditions, reducing strong adsorption to the RP C18 stationary phase and obtaining rapid and effective separation, the application of a RP C4 column resulted to be advantageous compared with RP C18. Using these conditions, the total ion current (TIC) chromatogram recorded for the butanol extract allowed to obtain a fair separation, ascertaining the major presence of ceramide and cerebroside compounds, close to minor galactolipid and phospholipid molecules (data not shown).

In order to improve the analysis conditions, the sample enriched in target molecules, obtained from the butanol extract of *D. loretense* corms, was analyzed by HPLC–ESI/ITMS, showing a chromatographic profile characterized by the occurrence of 21 ceramides and cerebrosides (Fig. 5).

Based on the knowledge of the fragmentation of the two standard substances, all 21 compounds were identified by HPLC–ESI/ITMS^n experiments (dracontioside A and B corresponding to compounds **5** and **14**, respectively), accomplished according to the conditions applied to the analysis of standard substances (Fig. 6). Thus, three main classes of ceramides and cerebrosides were represented, each one consisting of: – an hexose moiety, as carbohydrate headgroup in cerebroside species; – a saturated fatty acid, having a length from 16 to 26 carbon atoms and an hydroxy group in C2′, with the exception of compound **2**, made up of an hexadecanoic acid; – a previously described sphingoid base. Only compound **21** differed from the others for the occurrence of a 4-hydroxy-sphinganine long-chain base. In fact, the ESIMS^2 spectrum of the $[M-H]^-$ ion at *m*/*z* 682, along with two product ions at *m*/*z* 456 and 426 amu, corresponding to the neutral losses of a pentadecanal and a 2-hydroxy-hexadecanal molecule, respectively, clearly highlighted a peak ion at *m*/*z* 383, ascribable to 2-hydroxytetracosanoic acid ion, and due to the neutral loss of 299 amu, ascribable to a 1-dehydroxy-4-hydroxy-1-sphingenine unit. Accordingly, compound **21** was identified as the known 2-*N*-2′-hydroxytetracosanoyl-4-hydroxy-sphinganine ceramide, previously reported in *Russula cyanoxantha* [32].

The fingerprint product ion spectra obtained for each chromatographic peak observed in the TIC of *D. loretense* enriched sample permitted to unambiguously ascertain the presence, along with 14 known compounds, of 7 compounds never reported before (**4**, **7**, **10**, **11**, **13**, **15**, **18**) (Table 1). Noteworthy, product ion patterns of **15** and **18** firstly appeared very similar, showing a lot of peak ions with identical *m*/*z* values. However, the careful analysis of their respective ESIMS^n spectra allowed to ascertain that these product ions were only relative to the fatty acid moiety, alone or linked to a portion of sphingoid base (X, S, T, U, V ions), and thereby compounds **15** and **18** possessed the same fatty acid. On the contrary, the analysis of the product ions originating from the sphingoid base moiety showed a clear difference in the sphingoid skeleton of **15** and **18**, the former being a 4,8-sphingadienine able to form characteristic peak ions due to the neutral losses of 236 and 279 amu, and the second being a 4-hydroxy-8-sphingenine, giving rise to diagnostic $[(M-254)-H]^-$ and $[(M-297)-H]^-$ product ions.

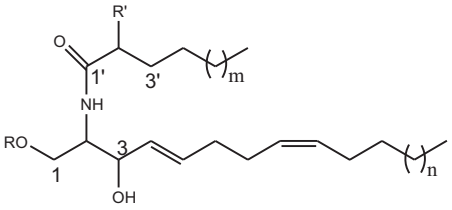

1: m = 11, n = 6, R = Glc, R' = OH [33]
4: m = 12, n = 6, R = Glc, R' = OH
5: m = 13, n = 6, R = Glc, R' = OH [30]
7: m = 14, n = 6, R = Glc, R' = OH
8: m = 15, n = 6, R = Glc, R' = OH [34]
10: m = 16, n = 6, R = Glc, R' = OH
11: m = 13, n = 6, R = H, R' = OH
12: m = 17, n = 6, R = Glc, R' = OH [35]
13: m = 14, n = 6, R = H, R' = OH
15: m = 15, n = 6, R = H, R' = OH
17: m = 19, n = 6, R = Glc, R' = OH [36]
20: m = 20, n = 6, R = Glc, R' = OH [37]

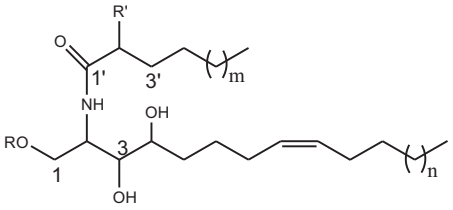

2: m = 11, n = 6, R = Glc, R' = H [38]
3: m = 13, n = 6, R = Glc, R' = OH [39]
6: m = 15, n = 6, R = Glc, R' = OH [39]
9: m = 17, n = 6, R = Glc, R' = OH [40]
14: m = 19, n = 6, R = Glc, R' = OH [31]
16: m = 20, n = 6, R = Glc, R' = OH [31]
18: m = 15, n = 6, R = H, R' = OH
19: m = 21, n = 6, R = Glc, R' = OH [31]

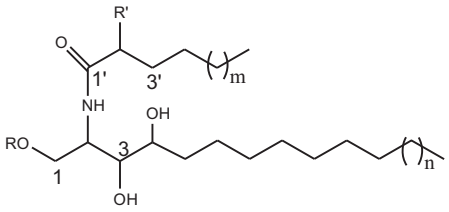

21: m = 19, n = 6, R = H, R' = OH [32]

Fig. 6. Ceramides and cerebrosides detected in HPLC–ESI/ITMS profile of *D. loretense* corms.

Table 1
ESIMS and ESIMS^n product ions of new ceramides and cerebrosides occurring in *D. loretense* corms.

	$[M-H]^-$	ESIMS^n product ions
4	726	708 $[(M-H_2O)-H]^-$, 564 $[(M-162)-H]^-$, 546 $[(M-180)-H]^-$, 534 $[(M-162-30)-H]^-$, 328 $[(M-162-236)-H]^-$, 327 (S), 311 (T), 285 $[(M-162-279)-H]^-$, 284 (U), 267 (V)
7	754	736 $[(M-H_2O)-H]^-$, 592 $[(M-162)-H]^-$, 574 $[(M-180)-H]^-$, 368 (X), 354 (S), 338 (T), 313 $[(M-162-279)-H]^-$, 295 (V)
10	782	764 $[(M-H_2O)-H]^-$, 620 $[(M-162)-H]^-$, 602 $[(M-180)-H]^-$, 590 $[(M-162-30)-H]^-$, 396 (X), 384 $[(M-162-236)-H]^-$, 382 (S), 366 (T), 341 $[(M-162-279)-H]^-$, 340 (U), 323 (V), 295 $[(M-279-46)-H]^-$
11	578	560 $[(M-H_2O)-H]^-$, 548 $[(M-30)-H]^-$, 354 (X), 342 $[(M-236)-H]^-$, 340 (S), 324 (T), 299 $[(M-279)-H]^-$, 298 (U), 281 (V), 253 $[(M-279-46)-H]^-$, 235 (P)
13	592	574 $[(M-H_2O)-H]^-$, 562 $[(M-30)-H]^-$, 368 (X), 356 $[(M-236)-H]^-$, 354 (S), 338 (T), 313 $[(M-279)-H]^-$, 312 (U), 295 (V), 267 $[(M-279-46)-H]^-$, 235 (P)
15	606	588 $[(M-H_2O)-H]^-$, 576 $[(M-30)-H]^-$, 382 (X), 370 $[(M-236)-H]^-$, 368 (S), 352 (T), 327 $[(M-279)-H]^-$, 326 (U), 309 (V), 281 $[(M-279-46)-H]^-$, 235 (P)
18	624	606 $[(M-H_2O)-H]^-$, 594 $[(M-30)-H]^-$, 382 (X), 370 $[(M-254)-H]^-$, 368 (S), 352 (T), 327 $[(M-297)-H]^-$, 326 (U), 309 (V), 281 $[(M-297-46)-H]^-$, 253 (P)

4. Conclusion

In the present study a prompt, selective, and sensitive analytical method to obtain qualitative on-line profiling of ceramides and cerebrosides occurring in *D. loretense* corms has been developed. The use of a preceding fractionation procedure, yielding sample enriched in target molecules, followed by an appropriate HPLC–ESI/ITMS^n method provided the unambiguous assignment of the structure of 21 ceramide and cerebroside species by fingerprint multistage mass spectra analysis, which allowed the rapid identification of 4,8-sphingadienine, 4-hydroxy-8-sphingenine and 4-hydroxy-sphinganine as the major long-chain bases, and of 11 different hydroxylated or not acyl-chain moieties as fatty acids. This HPLC–ESI/ITMS^n method provided high structure specific data for the determination of the exact pairing of fatty acids with long-chain bases and carbohydrate headgroups of ceramide and cerebroside compounds. Allowing the simultaneous characterization of known and unknown compounds, the method here reported, as well as to identify *D. loretense* corms as a promising source of bioactive sphingolipid compounds, could represent a reliable, sensitive, and simple approach to investigate new plant matrices looking for ceramide and cerebroside compounds. Besides, this study could represent a useful benchmark to develop a quantitative method to analyze sphingolipid compounds in plant matrices.

References

[1] P. Sperling, D. Warnecke, E. Heinz, Plant sphingolipids, in: G. Daum (Ed.), Lipid Metabolism and Membrane Biogenesis, Springer-Verlag, Berlin, Germany, 2004, pp. 337–380.
[2] R. Bittman, Z. Li, P. Samadder, G. Arthur, Anticancer activity of a ceramide analog containing a disulfide linkage, Cancer Lett. 251 (2007) 53–58.
[3] H. Oku, C. Li, M. Shimatani, H. Iwasaki, T. Toda, T. Okabe, H. Watanabe, Tumor specific cytotoxicity of β-glucosylceramide: structure–cytotoxicity relationship and anti-tumor activity in vivo, Cancer Chemother. Pharmacol. 64 (2009) 485–496.
[4] G. Lalazar, A. Ben Ya'acov, D.M. Livovsky, M. El Haj, O. Pappo, S. Preston, L. Zolotarov, Y. Ilan, β-Glycoglycosphingolipid-induced alterations of the STAT signaling pathways are dependent on CD1d and the lipid raft protein flotillin-2, Am. J. Pathol. 174 (2009) 1390–1399.
[5] K.T. Weber, D. Hammache, J. Fantini, B. Ganem, Synthesis of glycolipid analogues that disrupt binding of HIV-1 gp120 to galactosylceramide, Biorg. Med. Chem. Lett. 10 (2000) 1011–1014.
[6] J.H. Jung, C. Lee, Y.C. Kim, S.S. Kang, New bioactive cerebrosides from *Arisaema amurense*, J. Nat. Prod. 59 (1996) 319–322.
[7] H. Oku, S. Wongtangtintharn, H. Iwasaki, M. Inafuku, M. Shimatani, T. Toda, Tumor specific cytotoxicity of glucosylceramide, Cancer Chemother. Pharmacol. 60 (2007) 767–775.
[8] N.S. Radin, Designing anticancer drugs via the Achilles heel: ceramide, allylic ketones, and mitochondria, Bioorgan. Med. Chem. 11 (2003) 2123–2142.
[9] J.A. Shabbits, L.D. Mayer, High ceramide content liposomes with in vivo antitumor activity, Anticancer Res. 23 (2003) 3663–3669.
[10] S. Kim, M. Cho, T. Lee, S. Lee, H.-Y. Min, S.K. Lee, Design, synthesis, and preliminary biological evaluation of a novel triazole analogue of ceramide, Bioorg. Med. Chem. Lett. 17 (2007) 4584–4587.

[11] K.D. Kent, E.A. Clubbs, W.J. Harper, J.A. Bomser, Apoptotic effects on dietary and synthetic sphingolipids in androgen-independent (PC-3) prostate cancer cells, Lipids 43 (2008) 143–149.
[12] A. Benavides, A. Napolitano, C. Bassarello, V. Carbone, P. Gazzerro, A.M. Malfitano, P. Saggese, M. Bifulco, S. Piacente, C. Pizza, Oxylipins from *Dracontium loretense*, J. Nat. Prod. 72 (2009) 813–817.
[13] A. Brack Egg, Diccionario Enciclopedico de Plantas utiles del Perú, Centro de Estudios Regionales Andinos Bartolome de las Casas, Cuzco, Peru, 1999.
[14] M. Miyake, K. Sasaki, K. Ide, Y. Matsukura, K. Shijima, D. Fujiwara, Highly oligomeric procyanidins ameliorate experimental autoimmune encephalomyelitis via suppression of Th1 immunity, J. Immunol. 176 (2006) 5797–5804.
[15] E. Heinz, Plant glycolipids: structure, isolation and analysis, in: W.W. Christie (Ed.), Advances in Lipid Methodology, The Oily Press, Dundee, Scotland, 1996, pp. 211–332.
[16] T. Sugawara, T. Miyazawa, Separation and determination of glycolipids from edible plant sources by high-performance liquid chromatography and evaporative light-scattering detection, Lipids 34 (1999) 1231–1237.
[17] F. Fang, C.-T. Ho, S. Sang, R.T. Rosen, Determination of sphingolipids in nuts and seeds by a single quadrupole liquid chromatography–mass spectrometry method, J. Food Lipids 12 (2005) 327–343.
[18] H. Imai, M. Ohnishi, M. Kinoshita, M. Kojima, S. Ito, Structure and distribution of cerebroside containing unsaturated hydroxyl fatty acids in plant leaves, Biosci. Biotechnol. Biochem. 59 (1995) 1309–1313.
[19] J.E. Markham, J. Li, E.B. Cahoon, J.G. Jaworski, Separation and identification of major plant sphingolipid classes from leaves, J. Biol. Chem. 281 (2006) 22684–22694.
[20] A.H. Merrill Jr., M.C. Sullards, J.C. Allegood, S. Kelly, E. Wang, Sphingolipidomics: high-throughput, structure-specific, and quantitative analysis of sphingolipids by liquid chromatography tandem mass spectrometry, Methods 36 (2005) 207–224.
[21] J.E. Markham, J.G. Jaworski, Rapid measurement of sphingolipids from *Arabidopsis thaliana* by reversed-phase high-performance liquid chromatography coupled to electrospray ionization tandem mass spectrometry, Rapid Commun. Mass Spectrom. 21 (2007) 1304–1314.
[22] N. Bartke, A. Fischbeck, H.-U. Humpf, Analysis of sphingolipids in potatoes (*Solanum tuberosum* L.) and sweet potatoes (*Ipomoea batatas* (L.) Lam.) by reversed phase high-performance liquid chromatography electrospray ionization tandem mass spectrometry (HPLC–ESI-MS/MS), Mol. Nutr. Food Res. 50 (2006) 1201–1211.
[23] P. Norberg, R. Nilsson, S. Nyiredy, C. Liljenberg, Glucosylceramides of oat root plasma membranes – physicochemical behaviour in natural and in model systems, Biochim. Biophys. Acta 1299 (1996) 80–86.
[24] B.D. Whitaker, Cerebrosides in mature-green and red-ripe bell pepper and tomato fruits, Phytochemistry 42 (1996) 627–632.
[25] J. Adams, Q. Ann, Structure determination of sphingolipids by mass spectrometry, Mass Spectrom. Rev. 12 (1993) 51–85.
[26] Q. Ann, J. Adams, Structure determination of ceramides and neutral glycosphingolipids by collisional activation of $[M+Li]^+$ ions, J. Am. Soc. Mass Spectrom. 3 (1992) 260–263.
[27] Q. Ann, J. Adams, Structure-specific collision-induced fragmentations of ceramides cationized with alkali-metal ions, Anal. Chem. 65 (1993) 7–13.
[28] M.H. Lee, G.H. Lee, J.S. Yoo, Analysis of ceramides in cosmetics by reversed-phase liquid chromatography/electrospray ionization mass spectrometry with collision-induced dissociation, Rapid Commun. Mass Spectrom. 17 (2003) 64–75.
[29] M.L. Bandu, T. Grubbs, M. Kater, H. Desaire, Collision induced dissociation of alpha hydroxy acids: evidence of anion–neutral complex intermediate, Int. J. Mass Spectrom. 251 (2006) 40–46.
[30] H. Achenbach, M. Lottes, R. Waibel, G.A. Karikas, M.D. Correa, M.P. Gutpa, Alkaloids and other compounds from *Psychotria Correae*, Phytochemistry 38 (1995) 1537–1545.
[31] W.-K. Zhang, J.-K. Xub, X.-Q. Zhang, X.-S. Yao, W.-C. Ye, Sphingolipids with neuritogenic activity from *Euphorbia sororia*, Chem. Phys. Lipids 148 (2007) 77–83.
[32] J.M. Gao, Z.L. Dong, J.K. Liu, A new ceramide from the basidiomycete, Lipids 36 (2001) 175–180.
[33] B. Gzyl, M. Filek, A. Dudek, Influence of phytohormones on polar and hydrophobic parts of mixed phospholipid monolayers at water/air interface, J. Colloid Interf. Sci. 269 (2004) 153–157.
[34] P. Sperling, E. Heinz, Plant sphingolipids: structural diversity, biosynthesis, first genes and functions, Biochim. Biophys. Acta 1632 (2003) 1–15.
[35] X. Chen, Y.-L. Wu, D. Chen, Structure determination and synthesis of a new cerebroside isolated from the traditional Chinese medicine *Typhonium giganteum* Engl., Tetrahedron Lett. 43 (2002) 3529–3532.
[36] J. Ryu, J.S. Kim, S.S. Kang, Cerebrosides from *Longan Arillus*, Arch. Pharmacol. Res. 26 (2003) 138–142.
[37] E.B. Cahoon, D.V. Lynch, Analysis of glucocerebrosides of rye (*Secale cereale* L. cv Puma) leaf and plasma membrane, Plant Physiol. 95 (1991) 58–68.
[38] S.S. Kang, J.S. Kim, K.H. Son, H.P. Kim, H.W. Chang, Cyclooxygenase-2 inhibitory cerebrosides from *Phytolaccae radix*, Chem. Pharm. Bull. 49 (2001) 321–323.
[39] P. Tuntiwachwuttikul, Y. Pootaeng-On, P. Phansa, W.C. Taylor, Cerebrosides and a mononoacylgalactosylglycerol from *Clinacanthus nutans*, Chem. Pharm. Bull. 52 (2004) 27–32.
[40] F. Cateni, J. Zilic, G. Falsone, F. Hollan, F. Frausin, V. Scarcia, Preliminary biological assay on cerebroside mixture from *Euphorbia nicaeensis* All. Isolation and structure determination of five glucocerebrosides, Farmaco 58 (2003) 809–817.